



Contaminants of emerging concern (CECs) adsorption on superfine activated carbon

C. G. M. Fonseca ^{a,*}, A. Sartoratto^b, A. N. Ponezi^b, D. M. Morita^c and R. de L. Isaac ^a

^a Department of Infrastructure and Environment, School of Civil Engineering, Architecture, and Urban Design, University of Campinas – UNICAMP, Campinas, Sao Paulo 13083-889, Brazil

^b Biological and Agricultural Pluridisciplinary Research Center – CPQBA, University of Campinas – UNICAMP, Paulínia, Sao Paulo 13140-000, Brazil

^c Department of Hydraulic and Environmental Engineering, Polytechnic School, University of Sao Paulo – EPUSP, Sao Paulo 05508-010 Brazil

*Corresponding author. E-mail: fonseca@fec.unicamp.br

 CGMF, 0000-0002-0380-8588; R de LI, 0000-0002-8820-4141

ABSTRACT

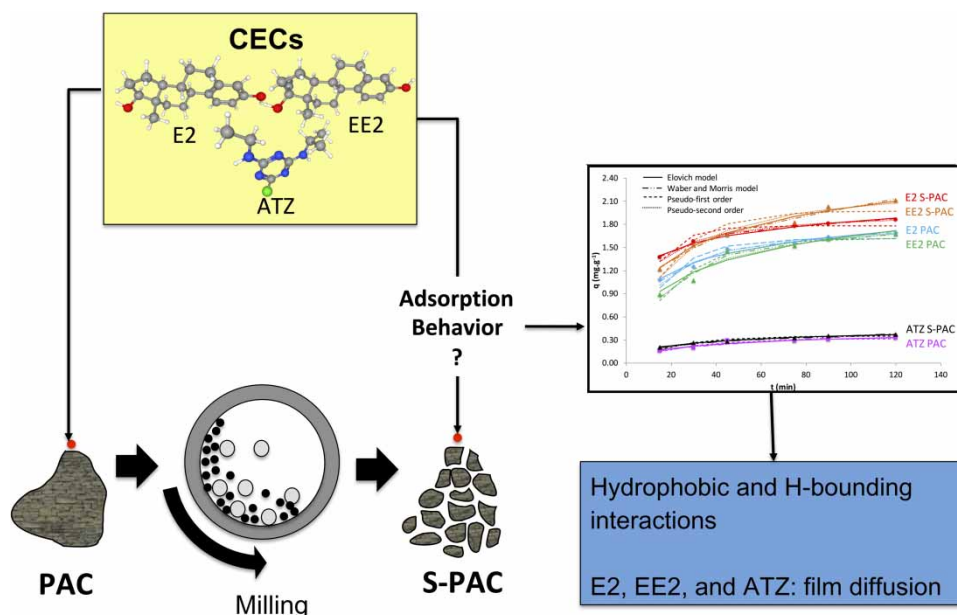
Contaminants of emerging concern (CECs) adsorption on superfine powdered activated carbon (S-PAC) (0.6 µm mean size) at conventional water treatment plants (WTP), where feasible contact time is usually shorter than 2 hours, was analyzed. Laboratory-scale experiments were carried out having deionized water (DW) and raw water (RW) samples fortified for atrazine (ATZ), 17β-estradiol (E2), and 17α-ethinylestradiol (EE2). Adsorption diminished due to natural organic matter, but in a smaller extension for S-PAC. Multi-solute removal efficiencies kept the same ranking for DW and RW, i.e., E2 > EE2 > ATZ, following compounds' hydrophobicity and molecular size. Hydrophobic and H-bonding interactions were the main adsorption mechanisms. For all target compounds the adsorption process was controlled by film diffusion. S-PAC presented higher adsorption as well as lower desorption as compared to powdered activated carbon, achieving similar efficiencies for half dosage and same contact time or at half contact time and same dosage. Physicochemical processes at WTP are capable to remove contaminated S-PAC particles.

Key words: 17α-ethinylestradiol, 17β-estradiol, adsorption, atrazine, superfine activated carbon, water treatment

HIGHLIGHTS

- S-PAC efficiencies are comparable to PAC at half contact time or dosage.
- After 2 hours (feasible at WTP), CECs removal increased up to 73%, for 10 mg/L S-PAC dosage.
- Elovich and Weber-Morris models fit target CECs adsorption kinetics on S-PAC.
- H-bonding rather than π -stacking interaction is the main adsorption mechanism.
- Physicochemical processes at WTP are capable to avoid contaminated S-PAC particles in tap water.

GRAPHICAL ABSTRACT



INTRODUCTION

Contaminants of emerging concern (CECs), such as pharmaceutical, personal care, agricultural, and veterinary products have been widely detected in several environmental matrices, such as wastewater, surface water, groundwater, and even drinking water. These compounds, although not regulated yet, have received increasing attention, namely from the U.S. Environmental Protection Agency (U.S. EPA), which publishes the Contaminant Candidate List (CCL) every five years, as result of the Safe Drinking Water Act (SDWA). These CECs are currently not subject to any proposed or promulgated national primary drinking water regulations but are known or anticipated to occur in public water systems. European Union has similar watch lists in the Water Framework Directive.

Physicochemical processes applied in conventional water treatment plants (WTP) have low efficiency on dissolved materials removal. Considering potential human health adverse effects associated with toxic, mutagenic, and/or endocrine-disrupting action, there is a growing search for processes capable to remove them at WTP avoiding their presence in drinking water, adsorption being the prevalent process. Researchers have tried to improve powdered activated carbon (PAC) performance by downsizing particles (Matsui *et al.* 2011; Matsui *et al.* 2013; Partlan *et al.* 2016, 2020; Nakayama *et al.* 2020). The characteristics and behavior of this so-called superfine activated carbon (S-PAC) are still little known.

S-PAC has shown to be a promising alternative, showing a higher adsorption capacity and faster kinetics than its precursor (Takaesu *et al.* 2019). Increase of available specific external surface area favors adsorption of large molecules; and decrease of hydrodynamic layer thickness surrounding the adsorbent particle facilitates external mass transfer or film diffusion, resulting in a faster transport into adsorption sites of small molecules (Partlan *et al.* 2016).

Adsorption performance depends on adsorbent physical and chemical characteristics, mainly surface functional groups' affinity to target compounds, pore size, and pore size distribution. Also, adsorption depends on adsorbates' properties, mainly molecule size, polarity, and hydrophobicity. Process performance is reliant on source water quality parameters, such as pH, temperature, and natural organic matter (NOM) that compete for adsorption sites, and WTP controlling adsorbent dosage, mixing, and contact time. While standard adsorption tests under lab conditions are usually led to equilibrium by keeping a quite high contact time, in full scale one can find just 2 hours or even less for total contact time whenever activated carbon is applied.

In a mixture of compounds, as in surface source waters subjected to anthropic action, competition occurs between target molecules and NOM affecting carbon adsorptive capacity. Decrease in adsorbent capacity of micropollutants removal is due

to at least two factors: direct competition for adsorption sites and internal pore obstruction, (Li *et al.* 2003). Even on background NOM presence, previous studies showed that S-PAC has a higher adsorption capacity than PAC (Matsui *et al.* 2010).

One important operating task when applying S-PAC at a full WTP refers to its removal from water afterward the adsorption step (Nakazawa *et al.* 2018, 2021). Since S-PAC size relays within that range of lowest particle removal efficiency by granular filtration when considering diffusion, interception, and sedimentation transport mechanisms, particle incorporation into flocs is essential for subsequent removal in settling tanks and granular filters.

The present work proposes to investigate S-PAC versus PAC performance on competitive adsorption of target CECs and NOM aiming to solve an environmental and health problem: their removal efficiency at conventional WTP and potential presence at trace levels in drinking water. Three environmentally relevant micropollutants were picked: atrazine (ATZ), 17 β -estradiol (E2), and 17 α -ethynylestradiol (EE2). The usual adsorption kinetics models were investigated, and complementary bench tests were carried out to verify S-PAC removal from treated water.

METHODS

Activated carbon

Commercial wood-based activated carbon (A800 Brascabo[®], BR) (Iodine number = 805 mg·g⁻¹ total ash = 6.85%; particles size = 91.2% <325 mesh; phenol index = 1.62 g·L⁻¹) was utilized. S-PAC was obtained from PAC by wet milling in a mortar and pestle. No dispersants were added for S-PAC production. After milling time (1 hour), milled S-PAC was placed in a ceramic dish and taken to a desiccator. Carbon samples were weighed out and inserted in 10 mL vials of deionized water, to get final dosages equals to 1.0, 2.5, 5.0, 10.0, and 25.0 mg·L⁻¹. The vials were sonicated for 10 min before use.

Adsorbent particle sizes were measured by dynamic light scattering in a Zetasizer Nano-ZS90 (Malvern Instruments Ltd., UK) after sonication for 1 minute within an ultrasonic bath. Surface area was calculated with Brunauer-Emmett-Teller (BET) equation and pore sizes distribution by BJH and t-plot methods, using N₂ gas adsorption data at 77 K temperature in an ASAP 2010 analyzer (Micromeritics[®], US). Adsorbents Zeta potentials were measured in a Zetasizer Nano-ZS90 device.

Adsorbates

E2 (hormone), EE2 (contraceptive), and ATZ (herbicide) (Sigma-Aldrich[®], US) were selected to study organic compound removal in an aqueous matrix by adsorption on laboratory scale. These specific compounds were chosen because of their worldwide occurrence in water sources in several urbanized and intensively farmed watersheds, the potential risk to human health, as well as their physicochemical properties, as shown in Table 1.

Initial concentrations of 6.70, 21.64, and 26.47 $\mu\text{g}\cdot\text{L}^{-1}$ for, respectively, ATZ, E2, and EE2 were adopted considering the limit of detection (LoD) and quantification (LoQ) of available analytical methods so that residual concentrations even after 99% removal were measurable. For this reason, initial concentration of CECs was fixed, and adsorbent dosage varied instead.

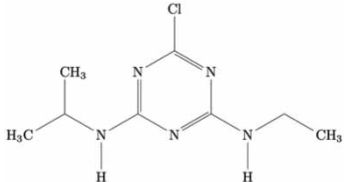
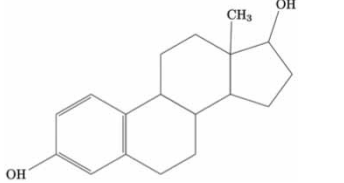
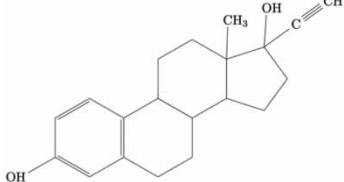
Adsorption bench experiments

Solid-phase extraction (SPE) cartridges C-18 (1,000 mg. 6 mL⁻¹, Applied Separations[®], USA) used for analytes concentration were conditioned, connected to a vacuum extraction system (Manifold, Alltech[®], England), passing 10 mL of methanol (HPLC Grade, JTBaker[®]) followed by 5 mL of ultrapure water (Milli-Q[®]) under low vacuum before running adsorption assays.

Deionized water (DW) samples were fortified for each compound in single-solute assays. Subsequently, tests were performed for analytes mixture (multi-solute assays), to look at the direct competition between target micropollutants. For analysis of adsorption process interference due to background NOM, raw water (RW) samples from Atibaia River, Sao Paulo State, Brazil (3.7 NTU turbidity, 6.2 mg·L⁻¹ TOC, 7.1 pH) were fortified with micropollutants mixture. Experiments were conducted twice for each experimental condition.

An activated carbon suspension was added to 5 out of 6 jars in jar-test apparatus (model 218-6LDB, Ethik[®], BR), each jar containing 2 L of water. Samples were shaken to keep activated carbon in suspension throughout the test (velocities gradient $G = 120 \text{ s}^{-1}$). Standard D3860-98 by American Society for Testing and Materials (ASTM) (temperature 20 °C, contact time 2 hours) were followed (ASTM 2020). After preset contact time was reached, samples underwent vacuum filtration through a 0.45 μm and then 0.2 μm cellulose acetate membrane (Analitica[®], BR; Sartorius Stedim Biotech GmbH 37070[®], GER, respectively) to remove residual activated carbon. Filtered samples were concentrated in C-18 cartridges. Cartridges were eluted with 20 mL of methanol at 1.0 mL·min⁻¹ flow rate. Eluted samples were evaporated to dryness via a rotary evaporator

Table 1 | Physicochemical properties of present work target compounds

Compound	CAS n ^a	MW ^a (g·mol ⁻¹)	log K _{ow} ^b	pK _a ^b	Water solubility ^a (mg·L ⁻¹ at 25 °C)	Molecular dimensions (Å×Å×Å)	Chemical Structure
ATZ	1912-24-9	215.69	2.61	<2	33.0	9.6 × 8.4 × 3.0 ^c	
E2	50-28-2	272.39	4.01	10.4	0.16–5.0	5.4 × 5.6 × 11.7 ^d	
EE2	57-63-6	296.41	3.67	10.5	11.3 ^e	6.5 × 5.6 × 12.1 ^d	

^aWesterhoff *et al.* (2005).^bYalkowsky *et al.* (2010).^cPelekani & Snoeyink (2001).^dSaha *et al.* (2010).^eWater solubility at 27 °C.

system (model R-215, Buchi[®], CH) and then re-suspended up to 2 mL in a volumetric flask with mobile-phase used in the chromatographic analyzes in a 60:40 volumetric ratio for water and acetonitrile (HPLC grade, JTBaker[®]). Samples were then transferred to vials to measure micropollutants residual concentrations in aqueous phase by high-performance liquid chromatography (HPLC) with diode array detector in Shimadzu LC-10A (Shimadzu[®], JP) equipped with SPD-10A UV-Visible detector (Shimadzu[®] Shim-pack CLC-ODS, JP). Linearity, precision, accuracy, LoD, and LoQ parameters were assessed for analytical method validation.

Adsorption kinetics

These experiments were performed by adding PAC or S-PAC (10.0 mg·L⁻¹) into 2 L jars containing RW spiked with mixed compounds at the same concentrations formerly applied. Samples were agitated at $G = 120 \text{ s}^{-1}$ in a temperature-controlled room ($20 \text{ °C} \pm 1$) and contact time from 15 to 120 minutes. Every experimental condition was carried out twice. Thus, each measurement refers to the average of results from duplicate assays.

To evaluate the results of the adsorption kinetic experiments, the most usual models were investigated: Elovich (Roginskii & Zeldovich (1934) *apud* Taylor & Thon (1952)); Weber and Morris model (Weber & Morris 1963); pseudo-first order (PFO) (Lagergren 1898), and pseudo-second order (PSO) (Blanchard *et al.* 1984).

The use of linearization in adsorption models may imply errors in the estimation of kinetic parameters. The ideal is to use non-linear models. Furthermore, it is known that, in most cases, the PFO equation is only applicable for the initial 20 or 30 minutes of contact time (Ho & McKay 1998). For these reasons, to obtain the kinetic parameters, the non-linear optimization technique was applied.

Evaluation of activated carbon removal through conventional water treatment

PAC and S-PAC suspensions were added to RW at 10 mg·L⁻¹ dosage. Coagulation/flocculation and sedimentation steps followed the methodology adopted by Nakazawa *et al.* (2018).

Activated carbon suspension was applied to every jar containing a 2 L volume sample solution, followed by coagulant addition (polyaluminium chloride, 10.5% Al_2O_3 , density equal to $1.2 \text{ g}\cdot\text{cm}^{-3}$) to get $3.34 \text{ mg Al}\cdot\text{L}^{-1}$. At the rapid-mix step, water sample was stirred for 1 min, followed by slow-mix performed under three steps of 10 min each at flocculation velocity gradients of 60 s^{-1} , 40 s^{-1} , and 20 s^{-1} . Sample was then put under quiescent conditions allowing flocs sedimentation. One aliquot was grabbed after 3.5 minutes (settling velocity $2 \text{ cm}\cdot\text{min}^{-1}$) for turbidity measurement (portable turbidimeter 2100N, Hach®, USA). Supernatant was filtered in filter paper, ashless, Grade 40, $8 \mu\text{m}$ (Whatman®, UK). Then, sample was subjected to membrane filtration on cellulose acetate, filter diameter 47 mm, $0.2 \mu\text{m}$ pore, (Sartorius Stedim Biotech GmbH 37070®, GER), and analyzed under optical microscopy. These sequential steps aimed to make paper filter break-through particles visible on cellulose acetate filter. Experiments were conducted twice for each experimental condition (Run 1 and Run 2). Investigation on remaining activated carbon particles for both sizes in filtered water was performed by comparing remaining turbidity results and analyzing membrane images by optical microscopy.

RESULTS AND DISCUSSION

Activated carbon characterization

PAC and S-PAC were characterized in terms of physicochemical properties, i.e., particle size, zeta potential, BET surface area, and pore size distribution (as percent related to total pore volume). Table 2 summarizes these results obtained.

Observed changes in BET surface areas from PAC to S-PAC were small (6.5%), agreeing to previous studies (Matsui *et al.* 2013; Partlan *et al.* 2016). Since the BET method considers the external and internal surfaces, particle downsizing brings out internal areas, keeping the total area practically the same. Results obtained regarding carbons pore size distribution are consistent with literature since there were no significant differences before and after milling. Researchers affirm that it is unlikely that the structural characteristics of internal pores will undergo major changes with pulverization (Matsui *et al.* 2011).

Competitive adsorption

Figure 1 allows visual comparison between removal efficiencies and residual concentrations of target compounds for single-solute (part a) and multi-solute (part b) experiments in DW, for each type of activated carbon and compound studied.

For multi- and single-solute assays, when higher dosages of activated carbon were applied ($\geq 10 \text{ mg}\cdot\text{L}^{-1}$), the adsorptive competition was practically not observed and the decrease in particle size did not influence adsorption. This fact can be explained by the adsorbents' sub-saturation under experimental conditions, evidenced by results obtained for lower carbon dosages ($\leq 5 \text{ mg}\cdot\text{L}^{-1}$) wherein competitive adsorption occurred showing removal efficiencies for multi-solute assays lower than those obtained for single-solute. For multi-solute conditions, although the specific surface area is close for PAC and S-PAC there was a greater influence of adsorbent particle size reduction, S-PAC being more efficient than PAC.

ATZ was the least adsorbed compound on both materials. This observation is in accordance with analytes hydrophobicity characteristics. Compounds having low $\log K_{ow}$ values tend to be more hydrophilic, making adsorption onto a carbon surface more difficult. While ATZ presents $\log K_{ow}$ equal to 2.61, E2 and EE2 present values of 4.01 and 3.67, respectively. Among the three target compounds, E2, which presents the higher $\log K_{ow}$ value, as expected presented the higher adsorption rate.

In addition to removal efficiency, residual concentration in the liquid phase must also be evaluated. Residual concentration values lower than $2 \mu\text{g}\cdot\text{L}^{-1}$ for ATZ were reached with a dosage equal to or higher than $10 \text{ mg}\cdot\text{L}^{-1}$ of PAC. Looking at S-PAC,

Table 2 | PAC and S-PAC characteristics

Properties	PAC	S-PAC
Particle size (average hydrodynamic diameter, μm)	1.70	0.60
Zeta potential (mV)	-20.2	-25.5
BET surface area ($\text{m}^2\cdot\text{g}^{-1}$)	599	560
Total pore volume - V_t ($\text{cm}^3\cdot\text{g}^{-1}$)	0.36	0.33
Micropore (% V_t): $17.5 \text{ \AA} < d_p < 20 \text{ \AA}$	59	60
Mesopore (% V_t): $20 \text{ \AA} < d_p < 500 \text{ \AA}$	38	36
Macropore (% V_t): $d_p > 500 \text{ \AA}$	3	4

Note: d_p = pore diameter.

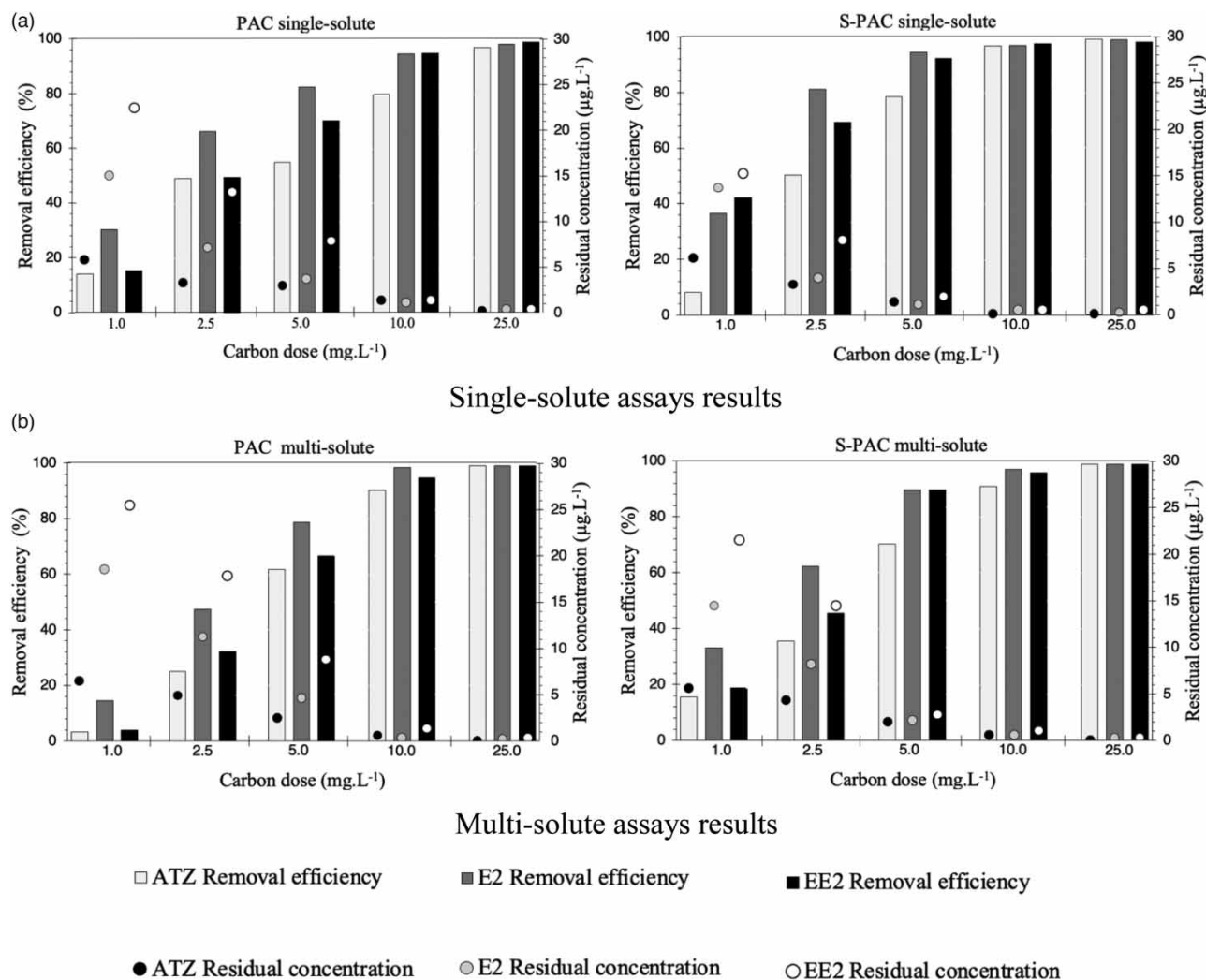


Figure 1 | CECs removal efficiency and residual concentrations for single-solute (part a) and multi-solute (part b) in DW for PAC and S-PAC.

this value was reached with half this dosage. For compound E2, it was observed that dosages equal to or greater than $5 \text{ mg}\cdot\text{L}^{-1}$ of PAC resulted in removal efficiencies greater than 80%. When S-PAC was used, efficiency close to this was already obtained for dosage equals to $2.5 \text{ mg}\cdot\text{L}^{-1}$. For EE2, similar behavior was observed (efficiencies around 70%). Thus, for higher carbon dosage used, comparing removal efficiencies obtained for PAC and S-PAC, it was observed that similar values were achieved by half S-PAC to PAC dosage.

Background NOM influence on the adsorption process was evaluated by comparing results obtained in RW and DW. The carbon dose used, i.e., $10 \text{ mg}\cdot\text{L}^{-1}$ was selected based on previous step. All samples were fortified with a mixture of considered analytes, and the contact time adopted was the same as in previous assays. The removal efficiency achieved in DW considering the PAC and S-PAC were, respectively, 90 and 91% for ATZ, 98 and 97% for E2, and 95 and 96% for EE2. In the RW assays, these values were 49 and 55% for ATZ, 78 and 86% for E2, and 63 and 80% for EE2, when applying the PAC and S-PAC, respectively.

Target compound adsorption for the RW matrix was lower than that observed for the DW matrix when considered the same type of carbon. During RW assays, due to other compounds' presence, such as organics, indicated by total organic carbon value ($\text{TOC} = 6.2 \text{ mg}\cdot\text{L}^{-1}$), it was noted a decrease in adsorbents performance, a negative effect of NOM content suggesting competition to adsorbents' active sites. Competitive adsorption between NOM and target organic contaminants was reported by diverse authors (Li *et al.* 2003; Yoon *et al.* 2003); Yoon *et al.* (2003) also suggest that NOM molecules block activated carbon pores, reducing the inner surface area available for adsorption.

S-PAC was more efficient for target compounds removal when compared to PAC. This finding may be explained by that shell adsorption mechanism proposed by Matsui *et al.* (2011, 2013) in which increasing adsorption capacity of large molecules, such as NOM, with the decrease in adsorbent particle size, is explained by increase in specific external surface area available. For small molecules, improvement in adsorption efficiency is attributed to a reduction in hydrodynamic layer surrounding adsorbent particle, facilitating the external mass transfer or the film diffusion.

The compounds' removal efficiency ranking ($E2 > EE2 > ATZ$) followed their $\log K_{ow}$ values. The lower ATZ adsorption as compared to the others may be related, besides its hydrophobicity, to NOM molecule size in the water matrix. As explained by Li *et al.* (2003), direct competition for adsorption sites occurs only in pores that are accessible to both NOM and organic micropollutants, and the latter generally have smaller molecular sizes. As a result, low molecular weight NOM components compete more effectively with these compounds for accessible pores. NOM molecules of higher molecular weight adsorb into larger pores, not competing for the same sites on activated carbon, but causing pore blockage. However, ATZ molecular weight and, beyond, molecular dimensions are comparable to those of target hormones (see Table 1) and, thus, NOM composition itself, not performed in present work, could not explain lower ATZ adsorption under such competitive conditions.

Adsorption kinetics

Figure 2 shows target compounds' residual concentration decay with time by PAC (part a) and S-PAC (part b) adsorption. One can note that adsorption is faster at the early stages of the process when there are many sites available, while it slows down towards equilibrium.

S-PAC had faster adsorption kinetics than the usual-size PAC, which favors its application in situations where the contact time is a limiting factor, as occurs at conventional WTPs.

Under experimental conditions studied, the adsorption rate of E2 was significantly higher than other compounds, and ATZ was the analyte having the slowest adsorption rate. As the adsorption kinetics followed the same trend already verified in the previous step ($E2 > EE2 > ATZ$), this behavior can be explained by the reasons already discussed (hydrophobicity and competitive adsorption).

S-PAC was more efficient in removing E2 and EE2 when compared to PAC. For ATZ, however, a significant difference was not observed when comparing both adsorbents performance. This compound presented the lowest removal efficiency, achieving, in the longest contact time studied, removals of 55 and 49%, for S-PAC and PAC, respectively. Removal of approximately 58% of E2 was achieved after 30 minutes for adsorption in S-PAC, while its PAC removal was only 41% at the same contact time. After 75 minutes for S-PAC, E2 efficiency removal was higher than 80%, and for PAC such removal was not obtained even after the longest contact time (i.e., 120 minutes).

Adsorptive capacity differences can be explained by competitive adsorption between target molecules and other compounds present in source water, measured as total organic carbon. Interference of other compounds, especially NOM, on CECs' adsorption, is widely reported in the literature (Pelekani & Snoeyink 2001; Li *et al.* 2003; Matsui *et al.* 2013).

Table 3 shows the R^2 values, obtained by comparison between experimental adsorption capacity values (q) and the values obtained in the models, for each target compound and adsorbent. All R^2 values were greater than 85% and therefore the models fit the experimental data, considering that the kinetics study was run with all compounds together in RW matrix.

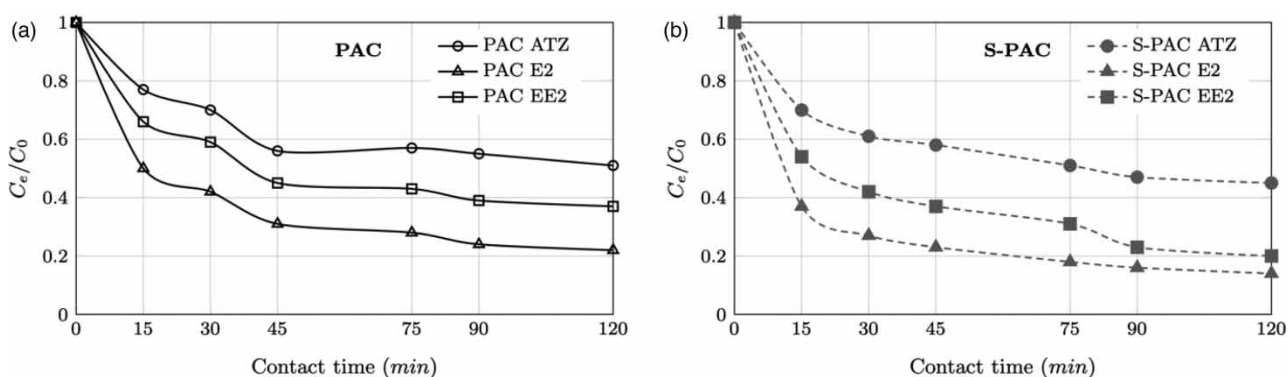


Figure 2 | Non-dimensional concentration variation as a function of contact time for target analytes in PAC (part a) and S-PAC (part b) (carbon dose = 10 mg·L⁻¹).

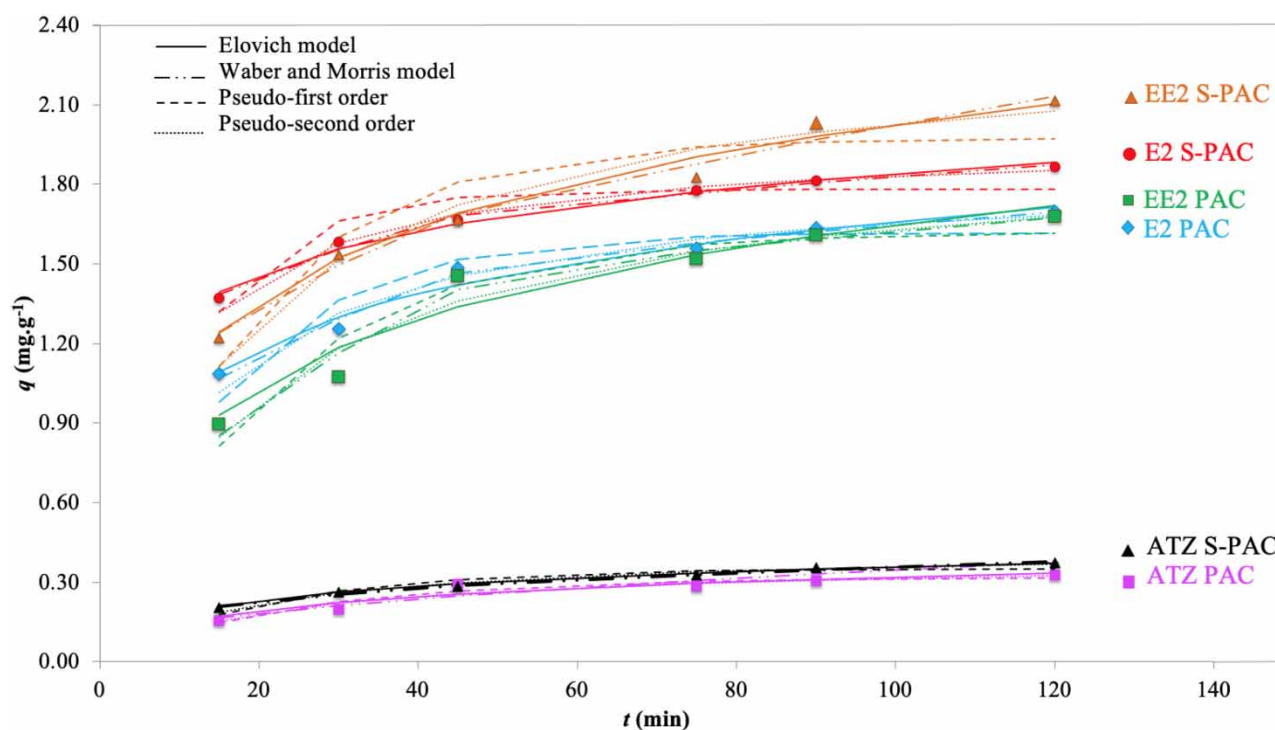
Table 3 | R^2 values obtained by comparison between experimental and model data

Model	Parameter	ATZ		E2		EE2	
		PAC	S-PAC	PAC	S-PAC	PAC	S-PAC
Elovich	α ($\text{mg}\cdot\text{g}^{-1}\cdot\text{min}$)	0.038	0.066	0.734	5.99	0.252	0.050
	β ($\text{mg}\cdot\text{g}^{-1}$)	12.077	12.392	3.311	4.266	2.529	2.361
	R^2	0.8994	0.9914	0.9747	0.9899	0.9449	0.9995
Weber and Morris	k_d ($\text{mg}\cdot\text{g}^{-1}\cdot\text{min}^{1/2}$)	0.024	0.023	0.087	0.067	0.113	0.123
	C ($\text{mg}\cdot\text{g}^{-1}$)	0.083	0.124	0.800	1.176	0.507	0.806
	R^2	0.8533	0.9803	0.9393	0.9418	0.9054	0.9722
Pseudo-first order equation	q_e ($\text{mg}\cdot\text{g}^{-1}$)	0.318	0.352	1.617	1.782	1.637	1.988
	K_1 (min^{-1})	0.040	0.0473	0.062	0.089	0.044	0.053
	R^2	0.9982	0.8939	0.8798	0.8545	0.9316	0.8633
Pseudo-second order equation	q_e ($\text{mg}\cdot\text{g}^{-1}$)	0.385	0.414	1.828	1.939	1.945	2.294
	K_2 ($\text{g}\cdot\text{mg}^{-1}\cdot\text{min}^{-1}$)	0.116	0.141	0.048	0.079	0.027	0.030
	R^2	0.9172	0.9679	0.9653	0.9877	0.9526	0.9543

Figure 3, containing adsorptive capacities as a function of time, displays the four studied kinetics models curves set for both adsorbents and target CECs.

The adsorption capacities of S-PAC in removing all target compounds were greater than the capacities of PAC. The ATZ, at the lower part of Figure 3, was the least adsorbed analyte in both PAC and S-PAC. Here the flat curves reveal the slowest adsorption rates of this analyte as compared to hormones.

The best fit to experimental kinetic data was obtained with the pseudo-second order equation, as the R^2 values were greater than 0.91 for all target compounds and adsorbents. However, as the pseudo-second order equation does not allow making any inference about the adsorption mechanisms (Tran *et al.* 2017) and the R^2 values were acceptable for both models (>0.85 , most >0.9), a specific study was carried out with the Elovich and Weber and Morris models.

**Figure 3** | Kinetics models curves for ATZ, E2 and EE2 adsorption on S-PAC and PAC.

Elovich model

The Elovich model is empirical and was initially developed to study the adsorption of carbon monoxide to finely divided MnO_2 (Roginskii & Zeldovich (1934) *apud* Taylor & Thon (1952)). It has been extensively applied, with success, to chemical adsorption of compounds from aqueous solutions (Cheung *et al.* 2001; Tseng *et al.* 2003; Wu *et al.* 2009). Furthermore, Ali *et al.* (2017) showed that Elovich's kinetic model was appropriate to describe the adsorption of E2 from water on iron nanoparticles and, Wang *et al.* (2020) concluded that the Elovich model better fit the experimental data of ATZ adsorption on peanut-shell biochar than both the pseudo first-order and pseudo second-order models.

Table 3 shows that the correlation coefficients were greater than 0.89 in all cases. One can see that α values follow the sequence $\text{E2} > \text{EE2} > \text{ATZ}$ for both adsorbents, which is consistent with decreasing $\log K_{ow}$ values (Table 1). The higher the $\log K_{ow}$ the more hydrophobic the compound and it will adsorb preferentially on hydrophobic surfaces as PAC or S-PAC. From these results, it seems that hydrophobic interactions are one of the main adsorption mechanisms for studied compounds.

ATZ, E2, and EE2 have aromatic rings in their structures (Table 1); however, the substituents are very different. ATZ has N and Cl as substituents in the aromatic ring so that they can act as π -acceptors. On the other hand, E2 and EE2 have OH as a substituent and may behave like π -donors. According to Haydar *et al.* (2003), among others, activated carbon surface has oxygen-containing groups, which influence aromatic compounds' adsorption since such groups act as π -donors. ATZ would be more adsorbed than both hormones, which is inconsistent with results obtained in the present work. Therefore, π -stacking interaction between aromatic π -systems in organic compounds and sorbents, cited by several researchers (e.g., Xiao & Pignatello 2015), is not the main adsorption mechanism in the present work.

Superficial oxygen-containing groups of activated carbon can form H-bonding with N – H of ATZ or OH of hormones. Since OH – OH bonds are more intense than OH – N – H, adsorption rates of E2 and EE2 must be higher than that of herbicide. In addition, steric hindrance due to atrazine side chains may prevent the binding of this compound to OH on the carbon surface. It should also be considered that oxygen-containing groups adsorb water via H-bonding, creating water clusters, which reduce aromatic compounds access, diminishing carbon adsorption capacity (Franz *et al.* 2000). This effect is more pronounced for ATZ. Therefore, one of the major adsorption mechanisms of target compounds studied in the present work can be the H-bonding interaction, cited by Villaescusa *et al.* (2011), Sophia & Lima (2018), among others.

The β values follow the order $\text{ATZ} > \text{E2} > \text{EE2}$, revealing that ATZ desorbs more than E2 and EE2. For ATZ, desorption rates β were very similar, however, the initial adsorption rate α on S-PAC was 1.7 times higher than on PAC. Although β value for E2 is 1.3 times higher with S-PAC than with PAC, α is eight times higher. For EE2, the value of α is five times greater for S-PAC than for PAC, and β values for PAC and S-PAC were similar. These results explain why S-PAC is better than PAC in the removal of target compounds.

Weber and Morris model

Table 3 presents the k_d and C values of Weber and Morris model for every target compound and adsorbent type. The correlation coefficients obtained in all the cases suggest that the model is adequate to describe ATZ, E2, and EE2 adsorption on PAC and S-PAC. According to Weber & Morris (1963), when the intra-particle diffusion controls the adsorption process, the variation of the quantity adsorbed (q) is linear with $t^{1/2}$. For Ho *et al.* (2000), if the plot doesn't pass through the origin, it is indicative of film diffusion control. For all conditions studied, the values of C are different from zero, showing that the process is controlled by film diffusion. The similarity in the k_d values for PAC and S-PAC, which have, respectively, particle diameters of 1.7 and 0.6 μm (Table 1), reinforces this conclusion. For the same contaminant and the same operating conditions, adsorbents with different particle diameters have different k_d values if the control mechanism is the intra-particle diffusion. When the PAC was milling, their inner pores were opened, the external surface area was increased and the number of internal adsorption sites was reduced, shortening the diffusion pathway. As the film diffusion controls the ATZ, E2, and EE2 adsorption, the performance of S-PAC was better than PAC. Researchers (e.g., Matsui *et al.* 2013) have proved that small adsorbates, such as geosmin and 2-methylisoborneol (MIB), also do not completely penetrate S-PAC, preferring to adsorb near the outer surface (shell adsorption).

Adsorbate molecular dimensions and adsorbent pore size distribution also influence adsorption (Pelekani & Snoeyink 2001). Pore size distribution was virtually unchanged after milling, 60% of pore diameter ranging from 17.5 to 20 Å and 40% from 20 to 500 Å. Furthermore, ATZ, E2, and EE2 molecules' dimensions are very similar (Table 1). Therefore, these

variables did not influence the adsorption capacity and kinetics of target compounds. The low concentrations of target CECs and NOM could explain the difficulty of access to the adsorbents' surfaces.

Comparison of PAC and S-PAC remaining after treatment

Turbidity values of samples collected after the WTP steps simulation revealed that maximum remaining turbidity in decanted water was, 2.5, 5.2, and 5.3 NTU for samples without carbon (control), and samples containing PAC or S-PAC, respectively, with no significant difference when comparing both adsorbents. For paper filtered water, the maximum remaining turbidity for control samples and PAC were 0.6 NTU, and 0.8 NTU for S-PAC. The difference of 33% between the turbidity values can be significant, being necessary to investigate this impact on the water quality in the future.

Filtering membranes used to simulate filtration in granular medium observed through optical microscope revealed a large removal of particles. It was observed little stains that would indicate activated carbon presence on membrane of 0.2 μm . As reported by Nakazawa *et al.* (2018), during membrane analysis it is difficult to distinguish between activated carbon particles and possible dark-colored minerals that may be present in RW. However, interference of those particles would be of small significance, since their concentration was much lower compared to carbon dosage (i.e., 10 $\text{mg}\cdot\text{L}^{-1}$).

Membrane surface examination by optical microscope combined to turbidity results indicate that PAC and S-PAC have been incorporated into the flocs, suggesting that they can be effectively removed by sedimentation and/or filtration. When using S-PAC as a substitute for PAC, the risk of some activated carbon particles passing through WTP processes and remaining in treated water does not increase substantially, as verified by Nakazawa *et al.* (2018). However, results obtained in the present work suggest that analytical methods must be developed to detect the difference between activated carbon and microflocs.

As adsorption constitutes a phase transfer process, CECs removed from RW remain on activated carbon as settling tank sludge and filter backwash water. Therefore, an assessment of the need for treatment of the WTP residues must be carried out before final disposal or beneficial use.

The present research was carried out in static reactors. The authors recommend pilot scale studies both to evaluate the removal of CECs in continuous flow reactors and thus the influence of hydrodynamic conditions, as well as to assess the removal of S-PAC in granular filters. By the precautionary principle, adsorption contributes not only to the removal of regulated compounds, such as ATZ, but also of CECs such as the hormones, improving safety of treated water for human consumption.

CECs adsorption on activated carbon can contribute to achieve goal #6 of 17 Sustainable Development Goals (SDGs), i.e., 'to ensure availability and sustainable management of water and sanitation for all' must be thought of not just for rural and small communities in developing countries but also for urbanized areas worldwide, mainly at those cities located in highly populated, industrialized, and agriculture watersheds where a huge amount of people live and wherever municipal water supply relies on reused surface waters. Safe drinking water involves application of the multiple barriers concept, those constituted by the unit processes and operations employed within the WTP itself, as well as other environmental management practices upstream, through green and gray structures for the water source's protection. In this scenario, a wide range of organic compounds occur. Since conventional WTPs are not able to properly deal with dissolved matter, advanced processes are needed to guarantee water safety. Adsorption preceded or not by oxidation, brings low construction costs, even at existing plants. On the other hand, operating costs related to adsorbents are usually high and process optimization is needed, especially regarding adsorbent type, dosage, and WTP point of application (contact time).

CONCLUSIONS

S-PAC performance was superior to PAC on target CECs (ATZ, E2, and EE2) removal from aqueous matrices (DW and RW) where competitive adsorption took place. Similar efficiencies were obtained at half contact time for the same dosage or even half dosage for the same contact time.

Analysis of results through Elovich's adsorption reaction model showed that *H*-bonding interaction is one of the main adsorption mechanisms of target compounds rather than π -stacking interaction between aromatic π -systems in organic compounds and sorbents. Initial adsorption rate (α) values follow decreasing $\log K_{ow}$ values, i.e., $E2 > EE2 > ATZ$ for both adsorbents, meaning that hydrophobic interaction is another adsorption mechanism of studied compounds. Higher values of α parameter explain why S-PAC was more efficient than PAC in target compounds removal.

According to Weber and Morris adsorption diffusion model, for all target compounds studied, the adsorption process is controlled by film diffusion. For this reason and as the inner pores of PAC are opened by milling, external surface area increases and the number of internal adsorption sites diminishes, shortening the diffusion pathway, S-PAC performance is better than PAC.

S-PAC particle size lies in that range of minimum efficiency removal by rapid granular filtration. However, bench-scale evaluation of activated carbon removal throughout coagulation-based physicochemical treatment and filtration showed that both adsorbents were incorporated into the flocs, indicating those particles can be fully removed by sedimentation and/or filtration, avoiding harmful presence in final water. S-PAC utilization is a promising strategy for optimizing organic compounds removal at conventional WTP, where feasible contact time is usually shorter than 2 hours, given the possibility of reducing dosage and/or required contact time when compared to conventional adsorbent (PAC) for some preset efficiency goal.

ACKNOWLEDGEMENTS

This study was financed in part by the Coordenação de Aperfeiçoamento de Pessoal de Nível Superior – Brasil (CAPES) - Finance Code 001; and Grant 2018/03294-9, Sao Paulo Research Foundation (FAPESP). This research used resources of the Brazilian Biosciences National Laboratory (LNBio), operated by the Brazilian Center for Research in Energy and Materials (CNPEM). Chromatographic analysis was run at Biological and Agricultural Pluridisciplinary Research Center (CPQBA), University of Campinas – UNICAMP.

CONFLICT OF INTEREST

The authors declare no conflict of interest.

DATA AVAILABILITY STATEMENT

All relevant data are included in the paper or its supplementary information.

REFERENCES

- Ali, I., Allothman, Z. A. & Alwarthan, A. 2017 [Supra molecular mechanism of the removal of 17- \$\beta\$ -estradiol endocrine disturbing pollutant from water on functionalized iron nano particles](#). *J. Mol. Liq.* **241**, 123–129. doi:10.1016/j.molliq.2017.06.005.
- ASTM 2020 *American Society for Testing Materials. D3860 – 98/2020. Standard Practice for Determination of Adsorptive Capacity of Activated Carbon by Aqueous Phase Isotherm Technique*. ASTM International City: West Conshohocken, PA, United States. doi: 10.1520/D3860-98R20.
- Blanchard, G., Maunay, M. & Martin, G. 1984 [Removal of heavy metals from waters by means of natural zeolites](#). *Water Res.* **18** (12), 1501–1507. doi:10.1016/0043-1354(84)90124-6.
- Cheung, C. W., Porter, J. F. & McKay, G. 2001 [Sorption kinetic analysis for the removal of cadmium ions from effluents using bone char](#). *Water Res.* **35** (3), 605–612. doi:10.1016/S0043-1354(00)00306-7.
- Franz, M., Arafat, H. A. & Pinto, N. G. 2000 [Effect of chemical surface heterogeneity on the adsorption mechanism of dissolved aromatics on activated carbon](#). *Carbon* **38** (13), 1807–1819. doi:10.1016/S0008-6223(00)00012-9.
- Haydar, S., Ferro-Garcia, M. A., Rivera-Utrilla, J. & Joly, J. P. 2003 [Adsorption of *p*-nitrophenol on an activated carbon with different oxidations](#). *Carbon* **41** (3), 387–395. doi:10.1016/S0008-6223(02)00344-5.
- Ho, Y. S. & McKay, G. 1998 [A comparison of chemisorption kinetic models applied to pollutant removal on various sorbents](#). *Process Saf. Environ. Prot.* **76** (4), 332–340. doi:10.1205/095758298529696.
- Ho, Y. S., Ng, J. C. Y. & McKay, G. 2000 [Kinetics of pollutant sorption by biosorbents: review](#). *Sep. Purif. Methods* **29** (2), 189–232. doi:10.1081/SPM-100100009.
- Lagergren, S. 1898 About the theory of so-called adsorption of soluble substances. *Kungliga Svenska Vetenskapsakademiens Handlingar* **24** (4), 1–39.
- Li, Q., Snoeyink, V. L., Mariñas, B. J. & Campos, C. 2003 [Elucidating competitive adsorption mechanisms of atrazine and NOM using model compounds](#). *Water Res.* **37** (4), 773–784. doi:10.1016/S0043-1354(02)00390-1.
- Matsui, Y., Nakano, Y., Hiroshi, H., Ando, N., Matsushita, T. & Ohno, K. 2010 [Geosmin and 2-methylisoborneol adsorption on super-powdered activated carbon in the presence of natural organic matter](#). *Water Sci. Technol. Water Supply* **62** (11), 2664–2668. doi:10.2166/wst.2010.415.
- Matsui, Y., Ando, N., Yoshida, T., Kurotobi, R., Matsushita, T. & Ohno, K. 2011 [Modeling high adsorption capacity and kinetics of organic macromolecules on super-powdered activated carbon](#). *Water Res.* **45** (4), 1720–1728. doi:10.1016/j.watres.2010.11.020.

- Matsui, Y., Nakao, S., Taniguchi, T. & Matsushita, T. 2013 Geosmin and 2-methylisoborneol removal using superfine powdered activated carbon: shell adsorption and branched-pore kinetic model analysis and optimal particle size. *Water Res.* **47** (8), 2873–2880. doi:10.1016/j.watres.2013.02.046.
- Nakayama, A., Sakamoto, A., Matsushita, T., Matsui, Y. & Shirasaki, N. 2020 Effects of pre, post, and simultaneous loading of natural organic matter on 2-methylisoborneol adsorption on superfine powdered activated carbon: reversibility and external pore-blocking. *Water Res.* **182**, 115992. doi:10.1016/j.watres.2020.115992.
- Nakazawa, Y., Matsui, Y., Hanamura, Y., Shinno, K., Shirasaki, N. & Matsushita, T. 2018 Identifying, counting, and characterizing superfine activated-carbon particles remaining after coagulation, sedimentation, and sand filtration. *Water Res.* **138**, 160–168. doi:10.1016/j.watres.2018.03.046.
- Nakazawa, Y., Abe, T., Matsui, Y., Shirasaki, N. & Matsushita, T. 2021 Stray particles as the source of residuals in sand filtrate: behavior of superfine powdered activated carbon particles in water treatment processes. *Water Res.* **190**, 116786. doi:10.1016/j.watres.2020.116786.
- Partlan, E., Davis, K., Ren, Y., Apul, O. G., Mefford, O. T., Karanfil, T. & Ladner, D. A. 2016 Effect of bead milling on chemical and physical characteristics of activated carbons pulverized to superfine sizes. *Water Res.* **89**, 161–170. doi:10.1016/j.watres.2015.11.041.
- Partlan, E., Ren, Y., Apul, O., Ladner, D. & Karanfil, T. 2020 Adsorption kinetics of synthetic organic contaminants onto superfine powdered activated carbon. *Chemosphere* **253**, 126628. doi:10.1016/j.chemosphere.2020.126628.
- Pelekani, C. & Snoeyink, V. L. 2001 A kinetic and equilibrium study of competitive adsorption between atrazine and Congo red dye on activated carbon: the importance of pore size distribution. *Carbon* **39** (1), 25–37. doi:10.1016/S0008-6223(00)00078-6.
- Roginskii, S. & Zeldovich, Y. 1934 *Acta Physicochimica (U.R.S.S.)* **1** (3/4), 554–595.
- Saha, B., Karounou, E. & Streat, M. 2010 Removal of 17 β -oestradiol and 17 α -ethynyl oestradiol from water by activated carbons and hypercrosslinked polymeric phases. *React. Funct. Polym.* **70** (8), 531–544. doi:10.1016/j.reactfunctpolym.2010.04.004.
- Sophia, C. A. & Lima, E. C. 2018 Removal of emerging contaminants from the environment by adsorption. *Ecotoxicol. Environ. Saf.* **150**, 1–17. doi:10.1016/j.ecoenv.2017.12.026.
- Takaesu, H., Matsui, Y., Nishimura, Y., Matsushita, T. & Shirasaki, N. 2019 Micro-milling super-fine powdered activated carbon decreases adsorption capacity by introducing oxygen/hydrogen-containing functional groups on carbon surface from water. *Water Res.* **155**, 66–75. doi:10.1016/j.watres.2019.02.019.
- Taylor, H. A. & Thon, N. 1952 *Kinetics of chemisorption. J. Am. Chem. Soc.* **74** (16), 4169–4173. doi:10.1021/ja01136a063.
- Tran, H. N., You, S.-J., Hosseini-Bandegharai, A. & Chao, H.-P. 2017 Mistakes and inconsistencies regarding adsorption of contaminants from aqueous solutions: a critical review. *Water Res.* **120**, 88–116. doi:10.1016/j.watres.2017.04.014.
- Tseng, R.-L., Wu, F.-C. & Juang, R.-S. 2003 Liquid-phase adsorption of dyes and phenols using pinewood-based activated carbons. *Carbon* **41** (3), 487–495. doi:10.1016/S0008-6223(02)00367-6.
- Villaescusa, I., Fiol, N., Poch, J., Bianchi, A. & Bazzicalupi, C. 2011 Mechanism of paracetamol removal by vegetable wastes: the contribution of π - π interactions, hydrogen bonding and hydrophobic effect. *Desalination* **270** (1–3), 135–142. doi:10.1016/j.desal.2010.11.037.
- Wang, P., Liu, X., Yu, B., Wu, X., Xu, J., Dong, F. & Zheng, Y. 2020 Characterization of peanut-shell biochar and the mechanisms underlying its sorption for atrazine and nicosulfuron in aqueous solution. *Sci. Total Environ.* **702**, 134767. doi:10.1016/j.scitotenv.2019.134767.
- Weber, W. J. & Morris, J. C. 1963 Kinetics of adsorption on carbon from solution. *J. Sanitary Eng. Div. ASCE* **89** (2), 31–60.
- Westerhoff, P., Yoon, Y., Snyder, S. & Wert, E. 2005 Fate of endocrine-disruptor, pharmaceutical, and personal care product chemicals during simulated drinking water treatment processes. *Environ. Sci. Technol.* **39** (17), 6649–6663. doi:10.1021/es0484799.
- Wu, F.-C., Tseng, R.-L. & Juang, R.-S. 2009 Characteristics of Elovich equation used for the analysis of adsorption kinetics in dye-chitosan systems. *Chem. Eng. J.* **150** (2–3), 366–373. doi:10.1016/j.cej.2009.01.014.
- Xiao, F. & Pignatello, J. J. 2015 $\pi + -\pi$ interactions between (hetero) aromatic amine cations and the graphitic surfaces of pyrogenic carbonaceous materials. *Environ. Sci. Technol.* **49** (2), 906–914. doi:10.1021/es5043029.
- Yalkowsky, S. H., He, Y. & Jain, P. 2010 *Handbook of Aqueous Solubility Data*, 2nd edn. CRC press. Taylor & Francis Group, Boca Raton, FL, United States. doi: 10.1201/EBK1439802458.
- Yoon, Y., Westerhoff, P., Snyder, S. A. & Esparza, M. 2003 HPLC-fluorescence detection and adsorption of bisphenol a, 17 β -estradiol, and 17 α -ethynyl estradiol on powdered activated carbon. *Water Res.* **37** (14), 3530–3537. doi:10.1016/S0043-1354(03)00239-2.

First received 29 November 2021; accepted in revised form 4 February 2022. Available online 18 February 2022